Shear design in concrete beams without transverse reinforcement – A comparative study

Citation:
Mak, M.W.T. and Lees, J.M. (2022) Shear design in concrete beams without transverse reinforcement – A comparative study. *Proceedings of the IABSE Symposium Prague 2022 – Challenges for Existing and Oncoming Structures. 25-27 May 2022*, 1374-1381. Prague, Czech Republic. https://doi.org/10.17863/CAM.80900

Version:
Accepted for publication

Mak, M.W.T. and Lees, J.M. (2022) Shear design in concrete beams without transverse reinforcement – A comparative study. *Proceedings of the IABSE Symposium Prague 2022 – Challenges for Existing and Oncoming Structures*. 25-27 May 2022, 1374-1381. Prague, Czech Republic. https://doi.org/10.17863/CAM.80900

Shear design in concrete beams without transverse reinforcement - A comparative study

Michele Win Tai Mak, Janet M. Lees

University of Cambridge, Cambridge, UK

Contact: mwtm2@cam.ac.uk

Abstract

In reinforced concrete structures without transverse reinforcement, the shear resistance relies on different internal resisting mechanisms and their interaction. The dependence of the overall load-bearing capacity upon different geometrical and mechanical parameters is complex. There is no unified theory that is universally accepted and certain aspects are still subject to scientific debate. The lack of agreement between theories has led to the development of different formulations and design provisions. The results of predictive models can vary significantly. In some instances, the limited accuracy can lead to safety risks. In other cases, it can lead to overly conservative design with increased economic and environmental costs. In this study on the shear resistance of reinforced concrete beams without transverse reinforcement, a comparison was carried out between analytical and experimental results. The data from laboratory tests were compared with the predictions from different formulations including those from the ACI 318, Eurocode 2, Simplified Modified Compression Field Theory, simplified Critical Shear Crack Theory, and Strut-and-Tie method. The findings of this study contribute to the development of safer and more sustainable infrastructure.

Keywords: Arch; compression; crack; tooth; optimisation; strut.

1 Introduction

The efficiency of our infrastructure network depends on the accuracy and precision of the models that are used to estimate its performance. Where the load bearing resistance can be predicted adequately, design and assessment can lead to structures that are fully utilised and safe. In cases where predictive models are unable to give satisfactory predictions, decisions must be made on the conservative side, increasing the cost and environmental footprint of infrastructure. Conversely, in rare cases where the level of conservatism is not sufficient, structural collapses can occur with serious societal consequences. Although structural failures are to be prevented, the type of failure associated with each limit state is a critical aspect that affects design and assessment decisions. Structures are typically designed to behave – and only theoretically fail – in a safe manner. This means that the attainment of the ultimate resistance of a structure should occur gradually, with clear signs of distress and visible deformations. Nevertheless, there are instances where failures can occur suddenly, without prior indication that a structure is in a critical state. This is typically the case of brittle failures. These considerations can help identify structural aspects that constitute a priority for the industry. The 'riddle of shear failure' is, among others, a critical example [1].

The behaviour of reinforced concrete structures subjected to shear is notoriously complex and depends on numerous factors. It is commonly accepted that the presence of transverse reinforcement fundamentally changes the shear behaviour of reinforced concrete. Structures with or without shear reinforcement can therefore be studied separately [1-2]. The latter case typically leads to more brittle failures. Common structural elements of this type include deep transfer elements, flat slabs, cut-and-cover tunnels and foundation elements [2]. The present study focusses on the shear behaviour of reinforced concrete beams without transverse reinforcement.

Building upon the early design approaches by Ritter [3] and Morsch [4], Kani [1] developed the basis for one of the first rational theories to describe the shear behaviour of reinforced concrete structures without transverse reinforcement. As the cracking pattern leads to the development of a comb-like structure, he identified two internal resisting mechanisms: the beam action, reliant on the resistance of the vertical concrete 'teeth', and the arch action, based on the residual resistance of a flow of inclined compressive stresses directed towards the supports, shaped like an internal arch. The agreement of theoretical considerations and experimental evidence confirmed that, among other parameters, the shear behaviour of beam elements depends heavily on the ratio between the shear span and the effective depth of the element. This dependence led to the development of the so called Kani's valley. This design space indicates that certain configurations of span and longitudinal reinforcement are more vulnerable to premature shear failure and are characterised by a more severe reduction in strength. These considerations are of fundamental importance when investigating shear in reinforced concrete and are the basis for the investigation presented in this paper.

The behaviour of reinforced concrete structures without shear reinforcement that are shear-critical is complex. Predicting their resistance with accuracy and precision is challenging. Although significant research efforts have been devoted over the last decades to the development of a rational and unified theory, there is still disagreement on some of the fundamental aspects that underpin existing theories [5-7]. This lack of consensus led to different approaches, models and formulations. The predictions can vary significantly, up to one order of magnitude in extreme cases [7]. Comparing experimental evidence with existing analytical models, their assumptions, formulations and results, can help identify areas within the design space where there are knowledge gaps or further improvement is necessary. Enhanced predictions can ultimately reduce the economic, environmental and societal costs associated with the uncertainty of existing models.

2 Predictive models

Several predictive models are available in the literature. Some of the existing approaches have similarities and can be grouped into categories, which are schematically shown in Fig. 1.

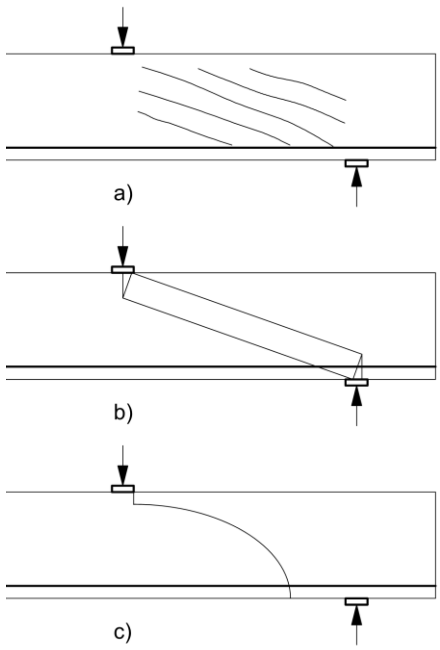

Figure 1. Different types of predictive models for reinforced concrete in shear: (a) Smeared crack; (b) Strut-and-Tie; (d) Discrete crack.

Design codes typically adopt a sectional approach, attributing a nominal shear resistance to the cross section of the element. Other models treat steel reinforced concrete as a continuum with different equivalent properties before and after cracking. This is done vie the concept of smeared cracking, which allows for the properties of the cracked concrete to be averaged. Other theories rely on the definition of an internal resisting load-path that is in equilibrium with the external forces and does not violate yield criteria. Such configurations are meant to represent an ultimate state of the structure, and reduction factors are applied on the material strength to take into account the detrimental effects of concrete cracking. Another class of theories focusses on the state of the structure after distributed cracking has localised, and failure is associated with the development of a single critical shear crack. For the purposes of this paper, only a few models and their formulations are recalled and compared in the following sections.

2.1.1 ACI sectional design

The American Concrete Institute (ACI) Building Code [8] includes a sectional shear design approach. An empirical equation for shear design was derived, corresponding to a lower threshold of the dataset from a large number of test results. The formulation for the concrete contribution V_c to the shear resistance is given by:

$$V_c = 0.17\Phi_c\sqrt{f'_c}b_w d \tag{1}$$

where f'_c is the concrete compressive strength in MPa, b_w is the effective width of the cross-section and d is its effective depth. Disregarding the initial empirical coefficient and the safety factor Φ_c, it can be noted that the resistance is associated with a nominal shear stress, which is a function of the square root of the concrete compressive strength. The formulation is of immediate applicability for design thanks to its simplicity, but does not take into account the dependence on any material parameter other than the concrete strength.

2.1.2 Eurocode 2 sectional design

In the Eurocode 2 [9], the shear resistance of a member without transverse reinforcement can be calculated based on a sectional design approach with the following formula:

$$V_{Rd,c} = C_{Rd,c}k(100\rho f_{ck})^{1/3}b_w d \geq 0.035k^{3/2}f_{ck}^{1/2} \tag{2}$$

$$C_{Rd,c} = \frac{0.18}{\gamma_c} \tag{3}$$

$$k = 1 + \sqrt{200/d} \leq 2.0 \tag{4}$$

$$\rho = A_{sl}/b_w d \leq 0.02 \tag{5}$$

where $C_{Rd,c}$ is an empirical coefficient with recommended values, k is a factor that takes into account size effects and a reduction in resistance as the structural depth increases, f_{ck} is the characteristic concrete cylinder strength and $\rho = A_s/bd$ is the longitudinal reinforcement ratio. An increase in resistance for higher reinforcement ratios is also taken into account.

2.1.3 Simplified Modified Compression Field Theory

The Modified Compression Field Theory (MCFT) [10] was developed based on tests on membrane concrete elements, considering concrete as a continuum even after cracking, but with different properties. It is therefore a theory of general applicability, and results on beam elements were used to validate its formulations, rather than calibrate them. It can however be computationally onerous and a Simplified Modified Compression Field Theory (SMCFT) [11] was developed for implementation in design codes, providing a sectional approach to shear design of more direct applicability. The calculations can be further simplified for elements under certain stress conditions, leading to the following formulation for elements without shear reinforcement:

$$v_c = \beta\sqrt{f'_c} \tag{6}$$

$$\beta = \frac{0.4}{1 + 1{,}500\varepsilon_x}\frac{1{,}300}{1{,}000 + s_{xe}} \tag{7}$$

$$\varepsilon_x = \frac{f_{sx}}{E_s} = \frac{v\ cot\theta - v_c/cot\theta}{E_s\rho_x} \tag{8}$$

$$s_{xe} = \frac{35s_x}{a_g + 16} \tag{9}$$

where β is the tensile stress factor in the cracked concrete, ε_x is the axial strain of the longitudinal reinforcement, s_{xe} is the crack spacing, s_x is the vertical distance between longitudinal reinforcement and a_g is the maximum aggregate size. In Equation 6 the first term in the denominator takes into account the strain effect and the second models the size effect. It can be noted that, even in this simplified formulation, the approach incorporates the dependence on several parameters.

2.1.4 Strut-and-Tie Model

A Strut-and-Tie Model [13] essentially consists in simplifying complex stress patterns into triangulated models based on a truss analogy: tension ties correspond to reinforcement bars in tension, compression struts correspond to concrete in compression, nodes are the intersection zones of struts and ties and they can be categorised based on the type of forces (tension or compression) acting on them. It can be used for the shear design of beam elements, with some limitations on the angle of the struts which can reduce their strength. Although this method has been incorporated in several design code with slightly different formulations and coefficients, in this example the reduction factors suggested by Schlaich et al. [6] are used on the design strength $f_{cd} = f_{ck}/\gamma_c$ to be applied on the nodes: $1.0\, f_{cd}$ for undisturbed compression; $0.8\, f_{cd}$ for nodes where tension reinforcement is anchored or crossing; $0.6\, f_{cd}$ for skew cracking or skew reinforcement; $0.8\, f_{cd}$ for skew cracks with extraordinary crack width.

2.1.5 Critical Shear Crack Theory

Theories such as the Critical Shear Crack Theory or the Critical Shear Displacement Theory assume that shear failure is associated with crack localisation. The load-carrying capacity is governed by a single critical crack and its ability to transfer shear forces. One key concept is aggregate interlock, that is the engagement of coarse aggregate in bearing across the discontinuity, activated by the relative slip of the two crack faces in the direction tangent to the crack. The Critical Shear Crack Theory [2] attributes the failure of a reinforced concrete beam to the development of one critical crack. As the width of the crack increases, the shear transfer through aggregate interlock across such a crack is lost, and this ultimately leads to failure. The generalised formulation is complex and can be solved iteratively. A few simplifications and assumptions allow for the derivation of a simplified closed-form expression [12], which can be used more directly for design purposes, leading to:

$$\frac{V_R}{b \cdot d} = 0.70 \cdot k_c^{2/3} \left(100 \cdot \rho \cdot f_c \frac{d_{dg}}{\sqrt{d \cdot a_{cs}}}\right)^{1/3}$$
$$k_c = \frac{1}{1 - 0.5 \cdot h_f / r_f} \tag{10}$$

where k_c takes into account the contribution of the compression zone, h_f which can be assumed equal to $0.3d$, r_f refers to the distance between the tip of the critical shear crack and the load acting on the compression face, and d_{dg} is a parameter related to the maximum aggregate size and a_{cs} refers to the moment-to-shear ratio at the control section.

3 Experimental programme

Laboratory tests were conducted to compare the predictions of the above-mentioned models with experimental results. Two reinforced concrete beams were tested in 3-point bending, with the same nominal geometry and properties, but different longitudinal reinforcement ratios. The main characteristics of the experiments are hereby described.

In many structural elements the type of loading is in principle unknown, and the concept of a defined shear span is often not directly relevant. Simplified code-based formulations therefore have to consider the most critical case possible, corresponding to the bottom of Kani's valley. This configuration, corresponding to a shear span-to-depth ratio of 2.5, was therefore adopted in the experimental programme, allowing for the majority of predictive models to be applied.

3.1.1 Geometry and Materials

The specimens were prismatic beams of length of 2,000 mm, a width of 160 mm and a height of 340 mm. The effective depth to the bottom reinforcement was 300 mm. The load and supports were positioned such that the shear span-to-depth ratio a/d was equal to 2.5. The bottom support plates had a length of 140 mm and a thickness of 10 mm, whereas the top central loading plate was 150 mm long and 34 mm thick. The clear distance between plates was therefore equal to 605 mm, resulting in a clear shear span-to-depth ratio of 2.02. The geometry of the specimen is shown in Fig. 2. The reinforcement consisted of two longitudinal deformed bars made of high-strength steel with a nominal yield strength of 500 MPa on the bottom tension side of the beams. The bars were 2H20 in specimen A (ρ = 1.31%) and 2H16 (ρ = 0.84%) in specimen B. No transverse reinforcement was present.

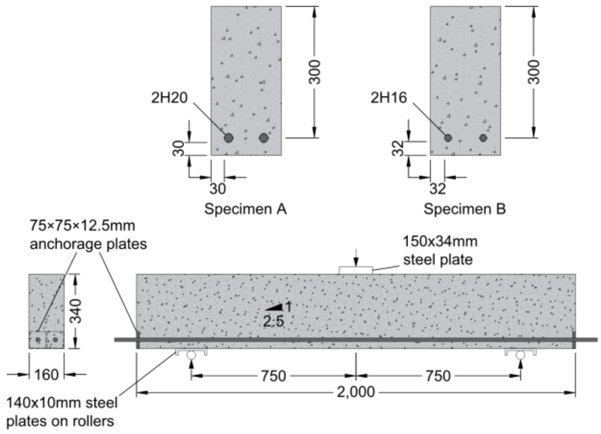

Figure 2. Geometry of the specimens.

The concrete was a High-Strength Ordinary Portland Cement (OPC) mix with no admixtures. The cement was a CEM I strength class 52.5N. Fine aggregate consisted of river sand; coarse aggregate was uncrushed coarse gravel with a maximum size of 10 mm. The mix composition and proportions of the constituents are given in Table 1. Material characterisation tests were carried out at 28 days after casting, at the same age of the structural load tests. Although the measured concrete strengths of the two beams differed slightly (see Table 1), on average the cylinder compressive strength (dia: 100 mm, height: 200 mm) was f_c = 47.6 MPa (SD: 4.68 MPa), the compressive strength measured on 100 mm concrete cubes was $f_{c,cub}$ = 62.5 MPa (SD: 1.56 MPa) and the split tensile strength measured on cylinders (dia: 100 mm, height: 200 mm) was $f_{ct,sp}$ = 4.24 MPa (SD: 0.48 MPa).

Table 1. Concrete composition

Constituent	Type	Density [kg/m3]	Amount [kg/m3]
Water	-	1,000	220
Cement	CEM I 52.5N	3,100	550
Fine aggregate	0/4	2,535	700
Coarse aggregate	4/10	2,535	855

The concrete was mixed in a planetary mixer with a capacity of 100 litres. The specimens were subsequently cast into plywood formwork, demoulded at least 24 hours after casting, covered in plastic sheets and left to cure in an indoor laboratory environment. The temperature and humidity during curing were not actively controlled or monitored. The companion cubic and cylindrical control specimens for material characterisation were cured underwater at ambient temperature.

3.1.2 Load-tests results

Specimen A with the greater reinforcement ratio of (ρ = 1.31%) failed at a shear force of 65.8 kN, whereas specimen B with less reinforcement (ρ = 0.84%) failed at a lower shear force of 60.9 kN. However, as shown in Table 2, the ultimate shear stress, normalised by the square root of the average concrete compressive strength of each specimen, was similar in both cases and equal to 0.190 √MPa.

Table 2. Summary of test results

Test	Reinf. ratio A_{sl}/bd [%]	Concrete strength f_c [MPa]	Shear force V_u [kN]	Norm. stress $V_u/bd\sqrt{f_c}$
A	1.31	51.9	65.8	0.1902
B	0.84	44.6	60.9	0.1900

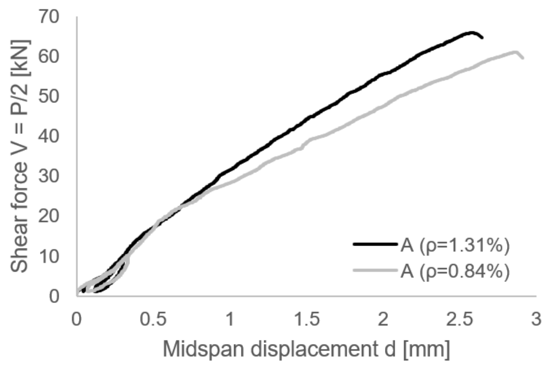

Figure 3. Load-deflection curves from the two tests

Fig. 3 indicates the load-deflection curves of the two tests. The load corresponds to the nominal shear force in the beams, equal to half the central point load, and the vertical displacement that was measured at midspan. The test on specimen A is indicated with a black line, whereas the test on the specimen B is shown in grey. Both specimens exhibited a similar behaviour. After an initial linear segment, the stiffness started to reduce at a displacement of approximately 0.5 mm and a shear force of approximately 15~20 kN. This corresponded to the development of cracking on the bottom tension side of the concrete. Subsequently, a progressive and limited reduction in stiffness occurred. Thus, the specimens continued to deform almost linearly, until a brittle failure occurred at a displacement of approximately 2.5~3.0 mm.

The cracking pattern of the two specimens after failure is shown in Figure 4. The outline of an assumed diagonal strut from the Strut-and-Tie Model is also shown with dashed white lines, for reference. The thin black lines indicate the final stage of the stable propagation of distributed cracking that developed as the external load increased. The analysis of the cracking pattern showed that the critical diagonal crack crossed the compression zone of the assumed diagonal strut before failure, at a load that was approximately 80% of the ultimate value. The presence of diagonal cracking within the strut based on a direct path from the load point of the support therefore did not immediately compromise the load-bearing capacity. In both tests, failure was ultimately associated with the unstable propagation of a critical S-shaped crack that initiated at the bottom zone of the beam, developed towards the compression zone at midspan and ultimately progressed as a delamination crack along the bottom reinforcement towards the support. The critical crack is indicated with a thick black line.

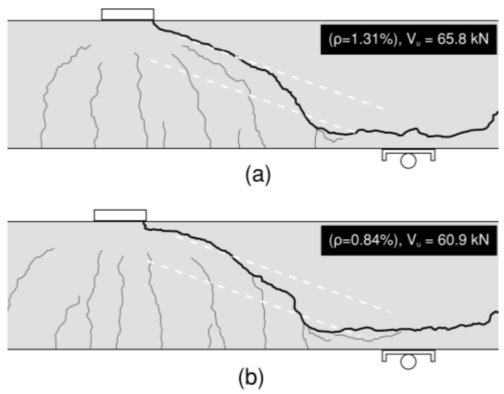

Figure 4. Cracking pattern after failure. Distributed cracking shown with thin black lines, critical cracks indicated with thick black lines, assumed diagonal strut shown with white dashed lines. (a) Specimen A with ρ=1.31%); (b) Specimen B with ρ=0.84%.

4 Comparison and discussion

A comparison between the experimental results and the analytical predictions based on the models described previously is shown in Fig. 5.

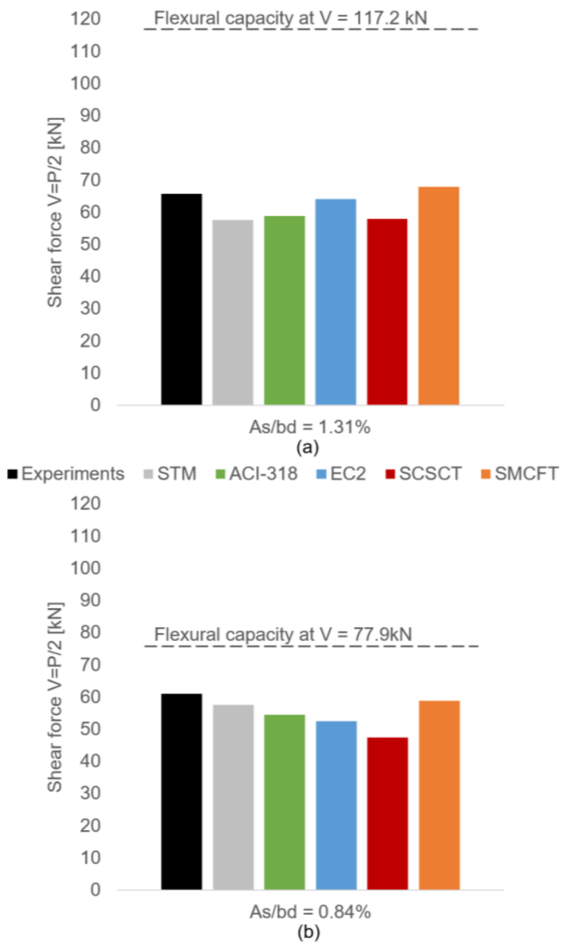

Figure 5. Comparison of shear capacity between experiments and predictive models based on Strut-and-Tie Model (STM), ACI-318, Eurocode 2 (EC2), Simplified Critical Shear Crack Theory (SCSCT), Simplified Modified Compression Field Theory (SMCFT): (a) Specimen A; (b) Specimen B.

It should be noted that safety factors equal to unity have been adopted in the calculations. In the case of specimen A with a greater amount of reinforcement, the majority of the models are reasonably accurate and the experimental-to-predicted shear strength ratios vary between 0.97 and 1.14. However in the STM the support node was predicted to limit the design and this was not observed in the experiment. In the second case of specimen B with less reinforcement, a greater scatter in the predictive results is obtained and the ratios vary between 1.04 and 1.28. Overall, the SMCFT was closer to the experimental results if both tests are considered. In the case of the STM, the predictions are reasonably close to the experimental values and conservative, which is to be expected from an equilibrium-based method, therefore based on the lower bound theorem of plasticity. Nevertheless, the model was governed by the support node at the bottom face in compression, although this was not the failure mode observed in the experiments, which exhibited limited plasticity. For reference, the shear force corresponding to the nominal ultimate flexural capacity at mid-span is indicated in Fig. 5 with dashed lines. The flexural capacities of the cross sections were calculated adopting an elastic-perfectly plastic behaviour of the steel reinforcement corresponding to the nominal strength of 500 MPa. For specimen A, the calculated flexural capacity was equal to 87.9 kNm, which corresponds to a shear force of 117.2 kN. For specimen B, the calculated flexural capacity was 57.7 kNm at a shear force of 76.9 kN. This suggests that the steel reinforcement did not reach its yield point and the cross sections remained below their plastic limit. In particular, the utilisation factor in bending of the midspan cross sections at shear failure was 56% for specimen A and 79% for specimen B. This was confirmed by the measurements from the strain gauges on the reinforcement.

The loading and support plates transfer concentrated vertical compressive stresses and providing a degree of restraint to horizontal strains through friction. They therefore provide a degree of confinement locally. It can be observed that cracking did not develop in the zones close to the plates, and the top of the critical cracks corresponds to the edge of the loading plate. Although the total shear span is calculated to the center of the plate, consistent with equilibrium considerations, a reduced span could be considered with respect to cracking. The evolution of the cracking pattern during the tests indicated a change in behaviour as the load increased. The stable propagation of cracks led to the development of distributed cracking, with an inclination that progressively reduced as the cracks extended towards the top compression zone of the beams. In this stage, the experimental observations appeared consistent with the assumption of a smeared crack model, and the specimens exhibited significant load-bearing capacity even if the cracks interfered with the assumed compression diagonal strut. At the ultimate state close to failure, the development of a single crack reflected the assumptions of theories based on a critical crack. During its unstable propagation, the critical crack also crossed the diagonal compressive strut path between the load and support. This possible resisting mechanism identified by the STM was therefore compromised by the cracking within the compression struts, and this effect is reflected in the models with appropriate reduction factors on the material strength. Nevertheless, the prediction was governed by the bottom node, which should have failed by crushing of the concrete at the interface with the supports. This failure mode was not observed in the tests and bearing pressures appeared to have stayed well below acceptable levels. Another aspect of the STM that could be further interrogated relates to the kinematics of the internal resisting truss. Relative displacements are necessary to develop the resisting mechanism and induce internal strains and distortional energy. Yet the strut-and-tie method is an equilibrium-based approach, therefore based on the lower-bound theorem of plasticity, according to which compatibility conditions can be disregarded. A sufficent ability to redistribute stresses is one of the assumptions of this approach, which may be questioned in the case of low-ductility concrete, no transverse reinforcement and a resisting mechanism with significant strain demand.

5 Conclusions

Two reinforced concrete beams without shear reinforcement were tested in 3-point bending with a shear span-to-depth ratio of 2.5. The reinforcement ratio A_s/bd was 1.31% in specimen A and 0.84% in specimen B. The results were compared with predictive models from literature. The following conclusions were drawn:

- The shear strength was 65.8 kN for specimen A and 60.9 kN for specimen B.

- Cracks propagated within the zone of an assumed diagonal compression strut that ran from the support to the loading point at a force of approximately 80% of the ultimate shear force.

- The analytical predictions were more accurate for specimen A and varied by 14%. The predictions for specimen B were characterised by greater scatter and varied by 28%.

- The experimental evidence reflected the assumptions of theories based on smeared crack and critical shear crack concepts at different stages of the tests.

- The characteristics of a Strut-and-Tie Model in terms of failure mode were not observed in the experiments

6 Acknowledgements

The authors are grateful to the members of the Structures Research Group of the University of Cambridge who contributed to the experimental work and the discussion of the results presented here. In particular, the assistance of Dr Pieter Desnerck for the load testing was much appreciated. The authors gratefully acknowledge the financial support of the United Kingdom Engineering and Physical Science Research Council (EPSRC) via the Fellowship 'Tailored Reinforced Concrete Infrastructure: Boosting the Innate Response to Chemical and Mechanical Threats' [EP/N017668/1].

7 References

[1] Kani GN. The riddle of shear failure and its solution. ACI Journal 1964 Apr 1 (Vol. 61, No. 4, pp. 441-468).

[2] Muttoni A, Fernández Ruiz M. Shear strength of members without transverse reinforcement as function of critical shear crack width. ACI Structural Journal. 2008;105:163-72.

[3] Ritter, W., 1899. "Die Bauweise Hennebique. III. Schluss." (German) [The Hennebique System – III. Conclusions]. Schweizerische Bauzeitung, (Vol. 33, No. 7, pp. 59–61).

[4] Mörsch, E., 1906. Der Eisenbetonbau, seine Theorie und Anwendung. (German) [Reinforced Concrete, Theory and Application]. Stuttgart: Verlag Von Konrad Wittwer

[5] Dönmez A, Bažant ZP. Critique of critical shear crack theory for fib Model Code articles on shear strength and size effect of reinforced concrete beams. Structural Concrete. 2019 Aug;20(4):1451-63.

[6] Kotsovos MD. Conflicts between reinforced concrete design assumptions and actual concrete behaviour. Proceedings of the Institution of Civil Engineers-Structures and Buildings. 2020 Dec 30:1-2.

[7] Collins MP, Bentz EC, Quach PT, Proestos GT. The challenge of predicting the shear strength of very thick slabs. Concrete International. 2015 Nov 1;37(11):29-37.

[8] ACI Committee. Building code requirements for structural concrete (ACI 318-19) and commentary. 2019 American Concrete Institute.

[9] EN B. 1-1: 2004: Eurocode 2: Design of concrete structures-Part 1-1: General rules and rules for buildings. British Standards Institution, London. 1992.

[10] Vecchio FJ, Collins MP. The modified compression-field theory for reinforced concrete elements subjected to shear. ACI Journal. 1986 Mar 1;83(2):219-31.

[11] Bentz EC, Vecchio FJ, Collins MP. Simplified modified compression field theory for calculating shear strength of reinforced concrete elements. ACI Structural Journal. 2006 Jul 1;103(4):614.

[12] Cavagnis F, Simões JT, Ruiz MF, Muttoni A. Shear strength of members without transverse reinforcement based on development of critical shear crack. ACI Structural Journal. 2020 Jan 1;117(1).

[13] Schlaich J, Schäfer K, Jennewein M. Towards a consistent design of structural concrete. PCI Journal. 1987 May 6;32(3):74-150.